Ollscoil na Gaillimhe
University of Galway

Provided by the author(s) and University of Galway in accordance with publisher policies. Please cite the published version when available.

Title	Design of experiments approach to provide enhanced glucose-oxidising enzyme electrode for membrane-less enzymatic fuel cells operating in human physiological fluids
Author(s)	Bennett, Richard; Osadebe, Isioma; Kumar, Rakesh; Ó Conghaile, Peter; Leech, Dónal
Publication Date	2018-03-30
Publication Information	Bennett, Richard, Osadebe, Isioma, Kumar, Rakesh, Conghaile, Peter Ó, & Leech, Dónal. (2018). Design of Experiments Approach to Provide Enhanced Glucose-oxidising Enzyme Electrode for Membrane-less Enzymatic Fuel Cells Operating in Human Physiological Fluids. Electroanalysis, 30(7), 1438-1445. doi: doi:10.1002/elan.201600402
Publisher	Wiley
Link to publisher's version	https://doi.org/10.1002/elan.201600402
Item record	http://hdl.handle.net/10379/14825
DOI	http://dx.doi.org/10.1002/elan.201600402

Downloaded 2024-04-27T22:16:48Z

Some rights reserved. For more information, please see the item record link above.

Design of experiments approach to provide enhanced glucose-oxidising enzyme electrode for membrane-less enzymatic fuel cells operating in human physiological fluids

*Richard Bennett, Isioma Osadebe, Rakesh Kumar, Peter Ó Conghaile, Dónal Leech**

School of Chemistry & Ryan Institute, National University of Ireland Galway, University Road, Galway, Ireland

* e-mail: donal.leech@nuigalway.ie

Received: ((will be filled in by the editorial staff))
Accepted: ((will be filled in by the editorial staff))

Abstract

Graphite electrodes are modified with a redox polymer, [Os(4,4′-dimethoxy-2,2′-bipyridine)$_2$(polyvinylimidazole)$_{10}$Cl]$^+$ ($E°'$ = −0.02 V vs Ag/AgCl (3M KCl), crosslinked with a flavin adenine dinucleotide glucose dehydrogenase and multi-walled carbon nanotubes for electrocatalytic oxidation of glucose. The enzyme electrodes provide 52% higher current density, 1.22 ± 0.1 mA cm^{-2} in 50 mM phosphate-buffered saline at 37 °C containing 5 mM glucose, when component amounts are optimised using a design of experiments approach compared to one-factor-at-a-time. Current densities of 0.84 ± 0.15 mA cm^{-2} were achieved in the presence of oxygen for these enzyme electrodes. Further analysis of the model allowed for altering of the electrode components while maintaining similar current densities, 0.78 ± 0.11 mA cm^{-2} with 34% less enzyme. Application of the cost-effective anodes in membrane-less enzymatic fuel cells is demonstrated by connection to cathodes prepared by co-immobilisation of [Os(2,2′-bipyridine)$_2$(polyvinylimidazole)$_{10}$Cl]$^+$ redox polymer, *Myrothecium verrucaria* bilirubin oxidase and multi-walled carbon nanotubes on graphite electrodes. Power densities of up to 285 µW cm^{-2}, 146 µW cm^{-2} and 60 µW cm^{-2} are achieved in pseudo-physiological buffer, artificial plasma and human plasma respectively, showing promise for *in vivo* or *ex vivo* power generation under these conditions.

Keywords: fuel cells; enzyme electrodes; glucose dehydrogenase; bilirubin oxidase; redox polymer

DOI: 10.1002/elan.((will be filled in by the editorial staff))

1. Introduction

Enzymatic fuel cells (EFCs) are electrochemical devices that utilise biocatalysts for conversion of chemical energy to electrical energy [1-3]. In EFCs, enzymes replace the conventional metal catalyst providing improved specificity towards reactions they catalyse [1, 4, 5] allowing for development of miniaturised, potentially implantable or portable, membrane-less EFCs through the elimination of the need for half-cell compartments and separating membranes [2-4, 6]. Enzyme catalysts operate under relatively mild conditions (20-40 °C, neutral pH), making them attractive for power generation *in vivo* utilising fuels and oxidants such as glucose and oxygen present in the bloodstream [7-9].

Redox polymer matrices for enzyme electrodes improve shuttling of electrons between active site and electrode surface, making electron transfer independent of orientation or proximity of the enzyme active site to the electrode surface, in comparison to that for direct electron-transfer mechanisms between enzyme and electrode [5, 10]. Current output from enzyme electrodes depends on selection of mediator with appropriate structure and suitable redox potential for rapid electron transfer between enzyme active site and electrode surface [11, 12]. Osmium-based mediators have been widely used [2, 13-15] owing to the ability to modulate the mediator redox potential of the central Os metal by using coordinating ligands, the relative stability of the resulting complexes in the Os(II)/Os(III) states, and because the hydrogel characteristics of redox-polymer films permit rapid mass and charge transport, thus generating substantial current signals [2, 16, 17]. The inclusion of multi-walled carbon nanotubes (MWCNTs) is one route towards improving glucose oxidation currents for enzyme electrodes prepared by crosslinking the nanomaterial with enzymes and osmium-based redox mediators [8, 18-20], attributed to improved retention of enzyme activity [21, 22]. Tsujimura *et al.* reported on similar bio anodes with magnesium oxide-templated mesoporous carbon as a support structure for hydrogels consisting of FADGDH and redox polymer [23].

We here report on optimisation of an enzyme electrode for glucose oxidation based on co-immobilisation of an [Os(4,4'- dimethoxy-2,2'-bipyridine)$_2$(poly-vinyl imidazole)$_{10}$Cl]$^+$ (Os(dmobpy)PVI) polymer, selected due to its lower redox potential, −0.02 V vs Ag/AgCl (3 M KCl), compared to our previous studies using [Os(4,4'- dimethyl-2,2'-bipyridine)$_2$(poly-vinylimidazole)$_{10}$Cl]$^+$ (Os(dmbpy)PVI), and an enzyme [22]. A flavin adenine dinucleotide dependent glucose dehydrogenase (FADGDH) enzyme is selected over glucose oxidase due

to its lack of reactivity with oxygen as co-substrate, for operation of an EFC in a membrane-less glucose/oxygen solution. Tremey *et al.* have shown improved performance of glucose oxidase in the presence of oxygen through mutation of the enzyme [24].

Enzyme electrode current output is dependent on the relative amount of components (osmium redox polymer, enzyme and MWCNTs) and optimisation is usually undertaken by varying one factor at a time. Kumar *et al.* [25] used a response surface design of experiment (DoE) methodology to optimise components used to construct enzyme electrodes. They reported a 32% increase in glucose oxidation current in comparison to that observed for enzyme electrodes optimised by varying of one factor at a time [25, 26].

Here we develop and validate a DoE methodology to optimise the enzyme electrode performance for current output under pseudo-physiological conditions (5 mM glucose, 50 mM phosphate buffered saline, PBS, pH 7.4, 37 °C). The DoE-optimised enzyme electrodes provide >50% improvement of glucose oxidation current density in absence of oxygen compared to previously reported values with the same components optimised using one-factor-at-a-time approach (OFAT) [22]. Tailoring of dropcoat amounts guided by contour plots from DoE software to include a lower amount of enzyme provides similar current density at 5 mM glucose concentrations while saving on enzyme amount required. Application of the selected anodes in membrane-less enzymatic fuel cells is demonstrated by connection to an oxygen-reducing *Myrothecium verrucaria* bilirubin oxidase-based cathode, operating in pseudo-physiological buffer, artificial plasma and human plasma respectively, showing promise for *in vivo* or *ex vivo* power generation under these conditions.

2. Experimental

2.1. Materials

All chemicals and biochemicals were purchased from Sigma-Aldrich, unless otherwise stated. The flavin dependent glucose dehydrogenase is from *Aspergillus sp*. (FADGDH 1.1.99.10, Sekisui, Cambridge, USA; product GLDE-70-1192). The *Myrothecium verrucaria* bilirubin oxidase (MvBOd) is provided by Amano Enzyme Inc. (Product BO-3, Nagoya, Japan). The MWCNTs (product 659258; Sigma-Aldrich) were pre-treated under reflux in concentrated nitric acid for 6 h and isolated by filtration. Polyethylene glycol diglycidyl ether (PEGDGE) was purchased from Sigma-Aldrich (average Mn ~ 526). All aqueous solutions unless

otherwise stated were prepared in Milli-Q water (18 MΩ cm). The [Os(4,4′-dimethoxy-2,2′-bipyridine)$_2$(polyvinylimidazole)$_{10}$Cl]$^+$ (Os(dmobpy)PVI) and [Os(2,2′-bipyridine)$_2$(polyvinylimidazole)$_{10}$Cl]$^+$ (Os(bpy)PVI) redox polymers were synthesised accoridng to literature procedures [27, 28].

2.2. Methods

2.2.1. Anode enzyme electrode preparation

Electrodes were prepared from graphite rods (Graphite store, USA, 3.0 mm diameter, NC001295) insulated with heat shrink tubing and the exposed disk polished on fine grit paper to create a geometric working surface area of 0.0707 cm^2. Enzyme electrode assembly was achieved by depositing appropriate volumes from 5 mg mL^{-1} redox polymer aqueous solution, 10 mg mL^{-1} FADGDH aqueous solution, 46 mg mL^{-1} aqueous dispersion of acid-treated MWCNTs and 2 µL of a 15 mg mL^{-1} PEGDGE aqueous solution on the surface of the graphite working electrode and allowing the deposition to dry for 24 h. The amount of each component of MWCNTs, Os(dmobpy)PVI and FADGDH added in the enzyme electrode preparation step is determined by the Design Expert Software (version 9, STAT-EASE Inc., Minneapolis, USA) using the low, central and high levels selected in Table 5.1.

2.2.2. Electrochemical measurements

Electrochemical tests were conducted using a CH Instrument 1030 multichannel potentiostat in a three electrode cell containing 50 mM phosphate buffer saline (PBS, 150 mM NaCl) pH 7.4, at 37 °C as electrolyte and a Ag/AgCl (3 M KCl) reference electrode, a graphite working electrode and a platinum mesh counter electrode (Goodfellow).

2.2.3. Fuel cell assembly and testing

The EFCs were constructed by combining anode enzyme electrodes with a previously described cathode [29], prepared as described for anode enzyme electrodes except using *Mv*BOd as enzyme, (Os(bpy)PVI) as redox polymer and a volume of the 46 mg mL^{-1} aqueous dispersion of acid-treated MWCNTs to provide 78 % w/w MWCNTs in the coating procedure. The EFC current and power densities were estimated from linear sweep

voltammetry (LSV) obtained at 1 mV s^{-1} and normalised to the geometric area of the current-limiting electrode.

Oxygen saturation was estimated, by using a dissolved oxygen electrode and meter (EUTech Instruments), to occur at approximately 0.22 mM O_2, achieved by bubbling oxygen into the solution. The artificial plasma contained uric acid (68.5 mg L^{-1}), ascorbic acid (9.5 mg L^{-1}), fructose (36 mg L^{-1}), lactose (5.5 mg L^{-1}), urea (267 mg L^{-1}), glucose (916.5 mg L^{-1}), cysteine (18 mg L^{-1}), sodium chloride (6.75 g L^{-1}), sodium bicarbonate (2.138 g L^{-1}), calcium sulfate (23.8 mg L^{-1}), magnesium sulfate (104.5 mg L^{-1}) and bovine serum albumin (7 g L^{-1}) [30].

3. Results and Discussion

Enzyme electrodes were initially modified through the co-immobilisation of Os(dmobpy)PVI redox polymer, FADGDH and MWCNTs, using a PEGDGE di-epoxide cross-linker on graphite electrode. Cyclic voltammetry (CV) is used to characterise the Os(II/III) transition for the Os(dmobpy)PVI in the enzyme electrode for the presence and absence of substrate. CVs recorded at 1 mV s^{-1} scan rate in the absence of glucose display oxidation and reduction peaks centred at −0.02 V vs Ag/AgCl, which is similar to the redox potential previously reported for the osmium polymer in solution and on electrode surface [16, 19, 31]. In the absence of substrate, peak currents vary linearly with scan rate at slow scan rates (< 20 mV s^{-1}), thereby indicating a surface-confined response. At high scan rates (> 20 mV s^{-1}), CVs display peak currents that scale linearly to the square roots of scan rates, which indicates semi-infinite diffusion control as expected for the formation of multi-layered films on electrode surface. The osmium surface coverage (Γ_{Os}) for the redox polymer is calculated by integrating the area under the peak for CVs recorded at slow scan rates, the Γ_{Os} is comparable to previously reported values in the presence of MWCNTs [19]. CV upon addition of glucose to the electrochemical cells, measured at slow scan rates, resulted in a sigmoidal-shaped response for enzyme electrodes (Figure 1), which is characteristic of an electrocatalytic (EC′) process. A shift of ~ 100 mV for the half-wave potential ($E_{1/2}$) of the sigmoidal-shaped catalytic wave for enzyme electrodes in the presence of glucose in comparison to that observed in the absence of glucose is observed. Others have reported that a shift indicates glucose substrate transport limitation and occurs for a mixed-case between kinetic- and substrate-limited conditions [32, 33].

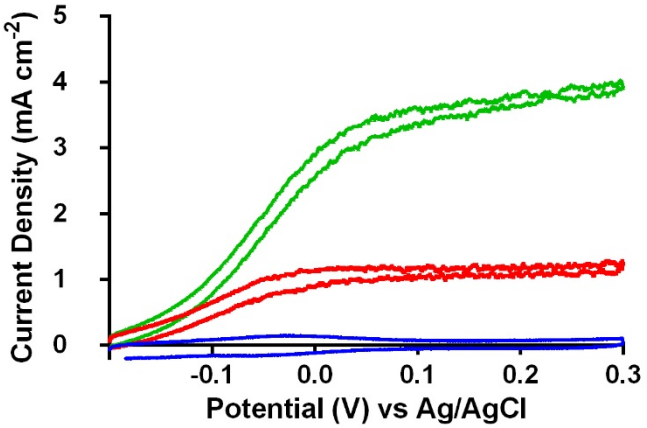

Figure 1 Slow scan rate, 1 mV s^{-1}, CV of Os(dmobpy)PVI (80 µg) films co-immobilised with FADGDH (100 µg) and MWCNTs (410 µg) in oxygen-free PBS containing no glucose (blue), 5 mM glucose (red) and 100 mM glucose (green) concentrations.

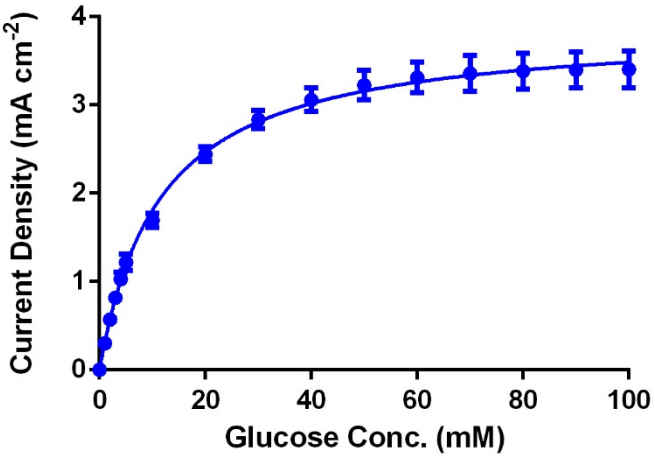

Figure 2 Glucose oxidation current densities as a function of glucose concentration, measured in oxygen-free PBS at 37 °C with stirring at 150 rpm at an applied potential of 0.15 V, for enzyme electrodes using Os(dmobpy)PVI (80 µg) co-immobilised with FADGDH (100 µg) and MWCNTs (410 µg).

Catalytic current densities for all anodes are extracted from steady state amperometry at an applied potential of 0.15 V, a potential selected to be in the region of the plateau current in the CV in the presence of 100 mM glucose (Figure 1) to ensure steady state current is achieved. Amperometric glucose oxidation current density is measured as a function of glucose concentrations (Figure 2). Amperometric current densities obtained are similar in magnitude to the catalytic plateau current densities observed with the slow-scan CV, thereby confirming steady state. An increase in glucose oxidation current density as a function of glucose concentration is observed, with substrate saturation at concentrations greater than 50

mM glucose for all enzyme electrodes. Apparent Michaelis-Menten constants, K_M^{app}, and maximum current densities j_{max} can be estimated using non-linear least squares to fit the amperometric plots to the Michaelis-Menten equation. The K_M^{app} of 16 ± 1 mM is obtained for enzyme electrodes co-immobilised with Os(dmobpy)PVI, MWCNTs and FADGDH and is similar to values obtained from previous report [19, 21].

3.1. Design of Experiment

For the optimisation of bioanodes, a DoE based on response surface factorial Box–Behnken Design (BBD) with a three level factorial design is used to evaluate the main effect and interaction between the MWCNTs, osmium redox polymer and FADGDH components required to prepare glucose-oxidising enzyme electrodes. The Box-Behnken design requires an experiment number according to $N = 2k\,(k - 1) + C_0$ [34], where k is the number of factors, and C_0 is the number of central points. The 16 run (with n=3 electrodes used to determine the current density for each run) experimental design is used to demonstrate the relative significance of the bioanode components and seek to enhance current density in pseudo-physiological conditions, compared to OFAT approach. The range and level of components investigated is given in Table 1 and runs and results used to build the model given in Table 2.

Table 1 The factors and levels selected to vary for DoE optimisation of performance of enzyme electrode.

Factor/Level	Low (−1)	Central (0)	High (+1)
MWCNTs (µg)	0	300	600
Os(dmobpy)PVI (µg)	10	55	100
FADGDH (µg)	20	60	100

Table 2 Design layout showing the run number, component level and the response (current densities in mA cm^{-2} measured amperometrically at 0.15 V vs Ag/AgCl in 5 mM glucose solution) and standard deviation (SD, n=3)

Run	Os(dmobpy)PVI	MWCNTs	FADGDH	Response	SD
1	−1	0	1	0.36	0.10
2	0	0	0	0.75	0.13
3	1	1	0	0.77	0.08
4	0	1	−1	0.58	0.04
5	0	0	0	0.85	0.10
6	−1	−1	0	0.23	0.08
7	0	−1	1	0.58	0.12
8	1	0	−1	0.63	0.14
9	−1	0	−1	0.21	0.07
10	0	0	0	0.70	0.10
11	0	−1	−1	0.39	0.05
12	1	0	1	0.79	0.11
13	1	−1	0	0.49	0.05
14	0	0	0	0.83	0.15
15	−1	1	0	0.14	0.05
16	0	1	1	0.87	0.24

The low levels of FADGDH and Os(dmobpy)PVI in this design are selected to be 20 µg and 10 µg respectively as a minimum level requirement for the production of glucose oxidation current density based on previous reports [2, 10, 14, 25, 35]. The high levels selected for each component are to eliminate difficulties in co-immobilisation and retention of higher amounts on electrode surface. For example, if higher amounts of the components are added, it is difficult to control the drop-coat on the electrode surface. The four runs for electrodes prepared using the central (0) component level, runs 2, 5, 10 and 14 in Table 2, achieve responses of 0.75 ± 0.13, 0.85 ± 0.10, 0.70 ± 0.10 and 0.83 ± 0.15 mA cm^{-2}, respectively, which, when all 12 electrode responses are considered together yield an average response of 0.77 ± 0.16 mA cm^{-2} for the central component level. Replication of the central levels strengthens the model. The response can be presented by a quadratic equation,

$$y = b_0 + b_1x_1 + b_2x_2 + b_3x_3 + b_{11}x_1^2 + b_{22}x_2^2 + b_{33}x_3^2 + b_{12}x_1x_2 + b_{13}x_1x_3 + b_{23}x_2x_3 \quad (1)$$

where y is the predicted current response value in mA cm^{-2}, x_1, x_2 and x_3 are the MWCNTs, redox polymer and enzyme amounts in µg used in the enzyme electrode preparation, b_0 is the constant coefficient (intercept), b_1, b_2, b_3 and b_{12}, b_{13}, b_{23} are linear and cross product coefficients, respectively, and the quadratic coefficients are b_{11}, b_{22} and b_{33}. The resulting response model from the 16 runs is

$$y = -0.15634 + 0.015719x_1 + 6.85648 \times 10^{-4}x_2 + 5.14236 \times 10^{-3}x_3 - 1.17901 \times 10^{-4}x_1^2 - 1.48611 \times 10^{-6}x_2^2 - 2.73438 \times 10^{-5}x_3^2 + 6.85185 \times 10^{-6}x_1x_2 + 1.38889 \times 10^{-6}x_1x_3 + 1.875 \times 10^{-6}x_2x_3 \quad (2)$$

In this response model, analysis of variance (ANOVA) is used for statistical testing and the data extracted demonstrates whether or not the model is statistically significant [36]. The low *F*-value (19.43) and p-value (0.0009) evaluated suggests that the model is statistically significant, as the higher the values, the more likely the rejection of the null hypothesis that the data show no variation. Furthermore, a coefficient of determination (R^2) between predicted and observed responses was evaluated to be 0.97, and when the amount of variation in the model was adjusted the measure of the adjusted R^2 (Adj R^2) value is 0.92, thereby suggesting significant correlation. These results are similar to those observed previously by Kumar *et al.* [25] for enzyme electrodes prepared by co-immobilisation of MWCNTs, GOx,

osmium redox complex and carboxymethylated dextran on graphite and current measured in physiological conditions.

3.2. Model Validation and Optimised Enzyme Electrode

In order for a system to be optimised, it is imperative to demonstrate that the model is a reasonable representation of the actual system and that it reproduces system behaviour with enough fidelity to satisfy analysis objectives. Model validation was tested based on values randomised by the model together with their predicted results under pseudo-physiological conditions (5 mM glucose, 50 mM phosphate buffered saline, PBS, pH 7.4, 37 °C), with the results presented in Table 3. A plot of predicted current density versus observed current density delivers a correlation (R^2) of 0.87 suggesting that the model is valid.

Table 3 Model validation comparing predicted versus actual (at 0.15 V) amperometric current density response for enzyme electrodes under pseudo-physiological conditions. Conditions as in Table 2. Errors are from the predicted standard deviation from the model for the predicted current density or from the standard deviation of 4 electrodes for the actual current density.

Os(dmobpy) PVI (μg)	MWCNTs (μg)	FADGDH (μg)	Predicted Current density mA cm^{-2}	Actual Current density mA cm^{-2}
56	316	63	0.80 ± 0.07	0.81 ± 0.05
100	316	63	0.78 ± 0.07	0.89 ± 0.04
100	600	63	0.81 ± 0.07	0.88 ± 0.07
100	600	97	0.88 ± 0.07	1.07 ± 0.13
100	600	26	0.67 ± 0.07	0.96 ± 0.09
100	291	26	0.64 ±0.07	0.78 ± 0.15
54	600	26	0.59 ± 0.07	0.60 ± 0.09
100	600	100	0.89 ±0.07	1.06 ± 0.27

Following the response achieved from enzyme electrodes prepared using this model, the FADGDH and MWCNTs amounts were shown to be the main factors contributing to the enhanced current densities (see Figure 3). A previous report has shown that the addition of MWCNTs on the enzyme electrode increased the amount of redox polymer that is co-immobilised and electronically coupled within the enzyme films leading to greater current

response [21]. Variation in the amount of the Os(dmobpy)PVI, once added, have the smallest effect of the three components.

The DoE optimum component amounts, based on maximising the predicted current density using equation 2, are 80 µg redox polymer, 410 µg MWCNTs and 100 µg FADGDH, predicted to deliver a current density of 0.93 ± 0.07 mA cm^{-2} in PBS containing 5 mM glucose. An actual measured current density of 1.22 ± 0.1 mA cm^{-2} (n=4) is obtained for the enzyme electrodes prepared using the DoE determined optimum component amounts. This represents a 52 % increase on the response, under similar conditions, for enzyme electrodes (0.8 mA cm^{-2}) using the same components and a OFAT method of optimisation of response [22].

The electrochemical response for the optimised enzyme electrodes is shown in Figure 1 and 2, demonstrating a maximum current density j_{max} of 3.41 ± 0.21 mA cm^{-2} for the electrode under glucose saturation (100 mM) conditions in comparison to previously reported j_{max} of 2.30 ± 0.31 mA cm^{-2} for the same enzyme electrode using the OFAT optimised component amounts.

Prior to incorporation of the optimised anode in a fuel cell setup a further round of testing was conducted based on consideration of the contour plot generated for FADGDH versus MWCNTs levels (Figure 3). The consideration of the contour plots and predicted response by variation in FADGDH and MWCNT amounts (Table 4) demonstrates that little variation in current density is observed in the region of 0.5 to 1.0 FADGDH and MWCNT levels (Figure 4). Thus the selected amounts for each of these factors can be altered depending on other factors to be considered in manufacturing enzyme electrodes, such as cost of materials or ease of electrode preparation.

Table 4 Predicted current densities from the model upon altering the amount of enzyme and MWCNTs on the electrode surface, using 80 µg for Os polymer. The errors are the predicted errors from the model.

MWCNTs (µg)	FADGDH (µg)	Predicted Current Density (mA cm^{-2})
410	100	0.93 ±0.07
500	100	0.93 ±0.07
600	100	0.91 ±0.07
410	80	0.90 ±0.07
500	64	0.87 ±0.07
540	64	0.86 ±0.07
600	64	0.86 ±0.07

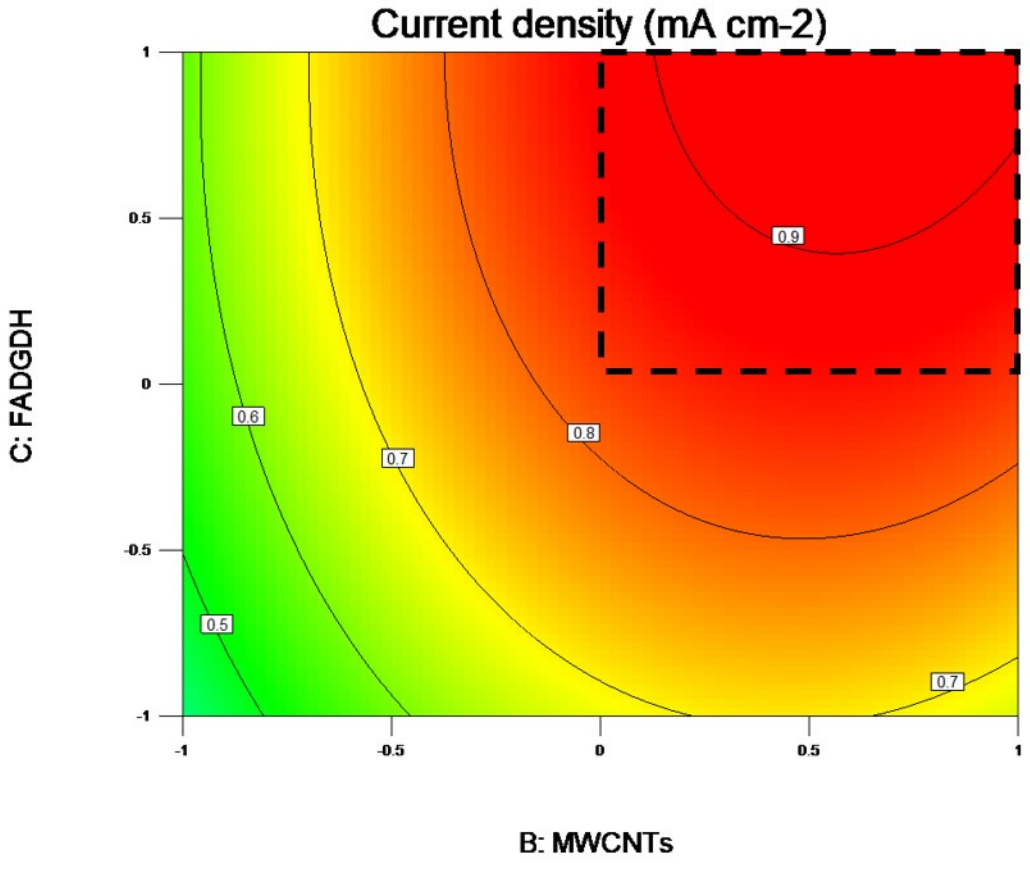

Figure 3 Contour plot for FADGDH vs MWCNTs showing glucose oxidation current density values predicted from the model (equation 2) attributed for each contour in mA cm^{-2}. The area outlined by the dotted black line shows relative component amounts that predict high current responses.

For example, use of lower amounts of enzyme makes the anode less expensive to produce while maintaining a high current response. A compromise amount of FADGDH of 64 µg and 540 µg of MWCNT is selected to maintain a high current response. This selected anode was used for fuel cell testing with component amounts of Os(dmobpy)PVI (80 µg), FADGDH (64 µg) and MWCNTs (540 µg) which is predicted to deliver 0.86 ± 0.07 mA cm^{-2}. Testing of the enzyme electrode anodes generated a current density of 1.0 ± 0.1 mA cm^{-2} (n=3) in 5 mM glucose solutions. These enzyme electrode anodes produce a maximum current density j_{max} of 2.63 ± 0.73 mA cm^{-2} in solutions of 100 mM glucose concentrations.

3.3. Operation in Oxygen

The selected bioanodes were further tested in the presence of oxygen in order to evaluate the effect of oxygen on these enzyme electrodes for eventual application in membrane-less EFCs. A 17% decrease in current density is observed for the enzyme electrode operating in 5 mM glucose concentration in the presence of oxygen, compared to the absence of oxygen, Figure 4. The decrease in glucose currents in the presence of oxygen suggests that molecular oxygen is reduced by the osmium redox polymer, which in turn decreases the amount of osmium redox centres that can be accessed by the electrons from glucose substrate, thus decreasing current density in the presence of oxygen, as reported on recently [16, 22, 37].

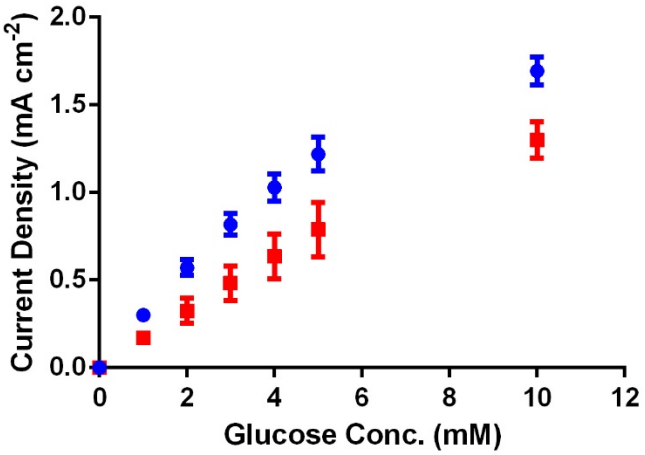

Figure 4 Glucose oxidation current density observed as a function of glucose concentration for the selected enzyme electrode (Os(dmobpy)PVI (80 µg) co-immobilised with FADGDH (100 µg) and MWCNTs (410 µg) measured in PBS at 37 °C with stirring at 150 rpm at an applied potential of 0.15 V, for enzyme electrodes in the presence (red) and absence of oxygen (blue).

3.3. Enzymatic Fuel Cell Testing

Enzymatic fuel cells were assembled based on the utilisation of glucose as fuel and oxygen as oxidant for testing under pseudo-physiological conditions using anodes prepared by co-immobilisation of Os(dmobpy)PVI redox polymers with FADGDH and MWCNTs using amounts optimised from the DoE approach. Enzyme electrodes chosen as cathodes are based on previous reports [22, 29] of Os(bpy)PVI redox polymer co-immobilised with *Mv*BOd and 78% w/w MWCNTs on graphite electrodes of the same geometric area as the anodes.

A potential application for EFC system is to power implantable medical devices via the oxidation of glucose as fuel and the reduction of oxygen as oxidant available in the bloodstream. Assembled EFC were therefore first tested in pseudo-physiological buffer conditions containing 0.2 mM O_2. For these EFCs, average power density of 270 ± 15 μW cm^{-2} is achieved (Figure 5) with a maximum power output of 285 μW cm^{-2}. The polarisation curves (Figure 6) for enzyme electrodes and the assembled EFC indicate that the cathode current density limits power produced. The maximum power density is observed at ~0.3 V similar to that obtained previously [22]. Others have reported on a membrane-less EFC operating at higher cell voltages. For example, Kim *et al.* [38] report on an EFC producing a power density of 50 μW cm^{-2} at a 0.5 V cell voltage under physiological conditions (air saturated pH 7.4, 140 mM NaCl, 37.5 °C in 15 mM glucose concentration) with the increased voltage due to the differences in redox potential of the osmium redox polymers selected. Due to differences in operating conditions, such as pH, glucose concentrations and also electrode preparation methodologies, comparison with other EFC results has proven difficult. Nonetheless our results compare well with those reported on for similar systems. For example, Soukharev *et al.* [39] report an EFC using GOx and a fungal laccase, co-immobilised with osmium redox polymers on 7 μm diameter, 2 cm long carbon fibres, produces a power density of 350 μW cm^{-2} in 15 mM glucose solutions. However, when the same EFC is tested for operation in 5 mM glucose solutions and using GOx sourced from *Penicillium pinophilum*, a power density of 280 μW cm^{-2} is achieved [40] similar to the maximum power density obtained in Figure 6. More recently MacAodha *et al.* [29] report on an EFC operating in pseudo-physiological conditions using a GDH enzyme but co-immobilised with Os(dmbpy)PVI redox polymer at the anode while *Myceliophthora*

thermophila laccase enzyme was used at the biocathode that produced a power density in in 5 mM glucose solutions of 145 µW cm^{-2}.

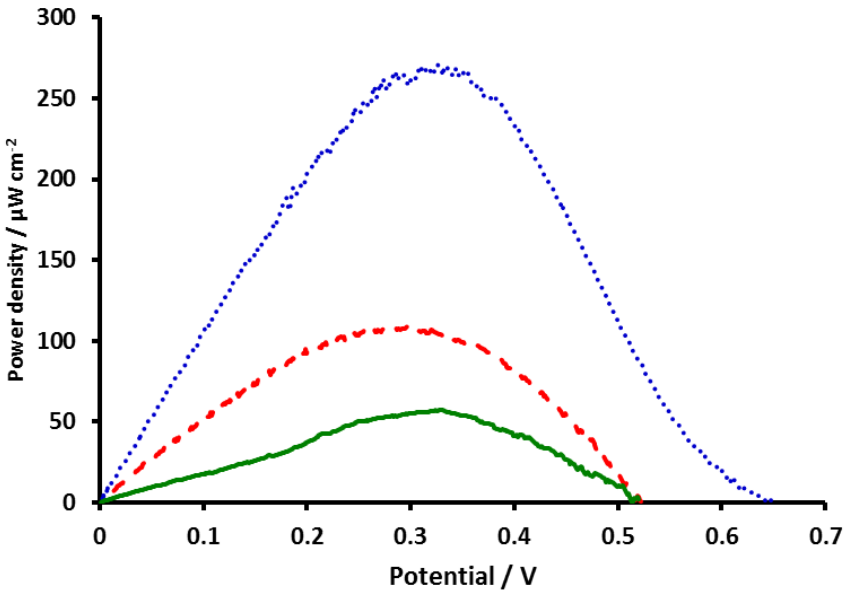

Figure 5 Power curves recorded for membrane-less enzymatic fuel cells using 1 mV s^{-1} linear sweep voltammetry in 50 mM PBS, at 37 °C, containing 5 mM glucose (blue dots), artificial plasma (red dash) and human plasma (green solid) for optimised bioanodes prepared by co-immobilisation of Os(dmobpy)PVI 80 µg with FADGDH 64 µg and MWCNTs 540 µg. Cathode enzyme electrodes prepared by co-immobilisation of Os(bpy)PVI, MWCNT and *Mv*BOd. Power densities normalised to the geometric area of the current-limiting electrode.

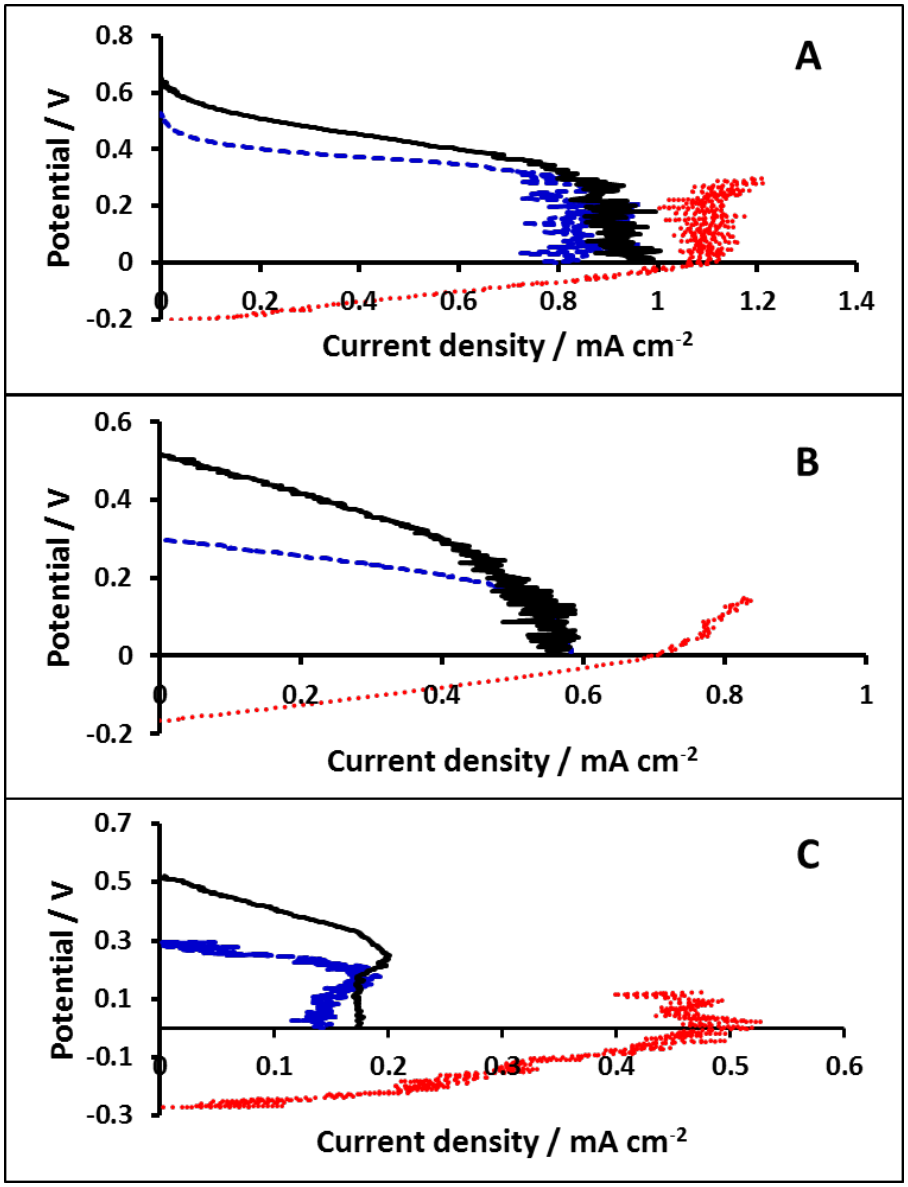

Figure 6 Polarisation curves from 1 mV s^{-1} linear sweep voltammetry recorded in 5 mM glucose and O_2 at 37 °C for optimised enzyme electrodes prepared by co-immobilisation of Os(dmobpy)PVI 80 µg co-immobilised with FADGDH 64 µg and MWCNTs 540 µg (red dotted line) as anodes and a cathode enzyme electrode prepared by co-immobilisation of *Mv*BOd and Os(bpy)PVI (blue dashed line) reported vs Ag/AgCl, and for the enzyme electrodes assembled as a membrane-less fuel cell (black solid line) operating in PBS (A), artificial plasma (B) and human plasma (C). Current densities normalised to electrode geometric area for anode and cathode and to the geometric area of the current-limiting electrode for the EFC.

To verify that EFC can produce power under more realistic sample conditions the assembled EFCs were operated in an artificial plasma recipe solution [30], providing an average power density of 109 ± 37 µW cm^{-2} (Figure 5) with a maximum power output of 146 µW cm^{-2}. Maximum power output produced in artificial plasma is approximately half that observed for the same EFC operating in PBS: a similar change has been reported by

MacAodha *et al.* achieving a power density of 60 µW cm^{-2} [29]. This difference in power output observed between artificial plasma and PBS is probably due to the presence of antioxidants and enzyme-inhibiting compounds in the artificial plasma solutions [41-43]. In addition, an oxygen concentration of only 0.06 mM was measured in the plasma, achieved by oxygen sparging through the solution, compared to 0.125 mM measured in the PBS. To evaluate the factors limiting the power output for the EFCs, polarisation curves at the anode and cathode enzyme electrodes from the 1 mV s^{-1} slow scan CVs can be combined to model cell polarisation curves for each EFC (see Figure 6). The polarisation curves indicate that the current at the cathode (as cathode and anode areas are the same) limits power produced at the assembled fuel cell under these conditions.

Further experiments were conducted to test for EFC operation in human plasma in an attempt to evaluate the effect of the deployment in real solutions. The human plasma sample was used as purchased. An average power density of 53 ± 9 µW cm^{-2} (Figure 6) with a maximum power output of 60 µW cm^{-2} is achieved for the EFC this sample. The maximum power output observed for human plasma is approximately half of that observed in artificial plasma. This difference is possibly due to the fact that blood plasma contains additional components such as blood clotting factors, lipids, hormones, enzymes, antibodies, and other proteins/components not present in artificial plasma, some of which are enzyme-inhibiting [44]. Although the oxygen concentration measured in human plasma is 0.1 mM and similar to a previous reported value [43, 45], the power density achieved is lower in comparison to that observed in artificial plasma which is most likely due to the effect the additional components in the plasma have on the cathode as the polarisation curves for the EFC (Figure 6) indicate that the cathode still limits the power produced in the EFC.

Others have reported on EFC operation in real samples. For example, an EFC based on direct electron transfer by cellobiose dehydrogenase enzyme at the anode and *Mv*BOd enzyme at the cathode was operated in human serum, human plasma and human blood samples [42], where no significant change in power output between PBS and real physiological solutions were observed, but a maximum power density of only 4 µW cm^{-2} obtained. A recent study on an EFC utilising FADGDH with a ferrocene redox hydrogel as bioanode and direct electron transfer at the biocathode using *Mv*BOd immobilised onto multi-walled carbon nanotubes modified with anthracene moieties reported power densities of ~58 µW cm^{-2} and ~45 µW cm^{-2} in human serum and citrate/phosphate buffer respectively at 37 °C [7]. Ó Conghaile *et al.* [45] report on an EFC constructed using enzyme electrodes of

Os(dmbpy)PVI, MWCNTs, and a de-glycosylated pyranose dehydrogenase at anodes and *Mv*BOd on a gold-nanoparticle modified electrode substrate as cathode. Power densities of up to 275 ± 50 μW cm^{-2} were achieved in pseudo physiological conditions, and 73 ± 7 μW cm^{-2} when tested in whole human blood [45, 46].

4. Conclusions

Enzyme electrode components were optimised using DoE methodology for application in physiologically relevant glucose solutions. Current densities of 1.22 ± 0.1 mA cm^{-2} were achieved at 5 mM glucose concentration in the absence of oxygen with 0.84 ± 0.15 mA cm^{-2} produced in the presence of oxygen. This represents a >50% increase on previously reported enzyme electrodes optimised using OFAT approach in absence of oxygen. Consideration of the model allowed for altering the electrode components to minimise cost while providing high current outputs. This suggests that at biologically relevant concentrations there is no precise optimal surface concentration but a range of values where high current outputs are achievable in the presence of oxygen. Further testing is required to provide a more robust model for current response. EFCs were assembled and tested for power generation to compare performances in oxygenated PBS, artificial plasma and human plasma using the optimised anode coupled to a cathode containing *Mv*BOd co-immobilised with Os(bpy)PVI and MWCNTs. The fuel cells were cathode limiting showing the need for further cathodic improvement to increase power output from the EFC. The assembled membrane-less EFCs produced power densities of 285 μW cm^{-2}, 146 μW cm^{-2} and 60 μW cm^{-2} in PBS, artificial plasma and human plasma respectively.

5. Acknowledgements

RB acknowledges support through an NUI Galway College of Science fellowship and an Irish Research Council postgraduate scholarship. IO acknowledges support through an NUI Galway College of Science fellowship. RK acknowledges support from the Earth and Natural Science Doctoral Studies Programme funded by the Higher Education Authority (HEA) through the Programme for Research at Third-Level Institutions, Cycle 5 (PRTLI-5) and co-funded by the European Regional Development Fund (ERDF). POC acknowledges support through a Science Foundation Ireland Technology Innovation Development Award.

5. References

[1] A. Heller, *Phys. Chem. Chem. Phys.* **2004**, *6*, 209.

[2] A. Heller, B. Feldman, *Acc. Chem. Res*. **2010**, *43*, 963.

[3] A. Heller, *AIChE J.* **2005**, *51*, 1054.

[4] S.C. Barton, J. Gallaway, P. Atanassov, *Chem. Rev*. **2004**, *104*, 4867.

[5] D. Leech, P. Kavanagh, W. Schuhmann, *Electrochim. Acta* **2012**, *84*, 223.

[6] T. Chen, S.C. Barton, G. Binyamin, Z. Gao, Y. Zhang, H.-H. Kim, A. Heller, *J. Am. Chem. Soc.* **2001**, *123*, 8630.

[7] R.D. Milton, K. Lim, D.P. Hickey, S.D. Minteer, *Bioelectrochem.* **2015**, *106*, 56.

[8] P. Ó Conghaile, D. MacAodha, B. Egan, P. Kavanagh, D. Leech, *J. Electrochem. Soc.* **2013**, *160*, G3165.

[9] S. Tsujimura, M. Fujita, H. Tatsumi, K. Kano, T. Ikeda, *Phys. Chem. Chem. Phys.* **2001**, *3*, 1331.

[10] A. Heller, *Phys. Chem. Chem. Phys.* **2004**, *6*, 209.

[11] A.E.G. Cass, G. Davis, G.D. Francis, H.A.O. Hill, W.J. Aston, I.J. Higgins, E.V. Plotkin, L.D.L. Scott, A.P.F. Turner, *Anal. Chem.* **1984**, *56*, 667.

[12] S.M. Zakeeruddin, D.M. Fraser, M.K. Nazeeruddin, M. Grätzel, *J. Electroanal. Chem.* **1992**, *337*, 253.

[13] Y. Ackermann, D.A. Guschin, K. Eckhard, S. Shleev, W. Schuhmann, *Electrochem. Comm.* **2010**, *12*, 640.

[14] F. Mao, N. Mano, A. Heller, *J. Am. Chem. Soc.* **2003**, *125*, 4951.

[15] M.D. Scanlon, U. Salaj-Kosla, S. Belochapkine, D. MacAodha, D. Leech, Y. Ding, E. Magner, *Langmuir* **2011**, *28*, 2251.

[16] A. Prévoteau, N. Mano, *Electrochim. Acta* **2013**, *112*, 318.

[17] D. MacAodha, M.L. Ferrer, P. O'Conghaile, P. Kavanagh, D. Leech, *Phys. Chem. Chem. Phys.* **2012**, *14*, 14667.

[18] B. Reuillard, A. Le Goff, C. Agnes, M. Holzinger, A. Zebda, C. Gondran, K. Elouarzaki, S. Cosnier, *Phys. Chem. Chem. Phys.* **2013**, *15*, 4892.

[19] D. MacAodha, P. Ó Conghaile, B. Egan, P. Kavanagh, C. Sygmund, R. Ludwig, D. Leech, *Electroanalysis* **2013**, *25*, 94.

[20] P. Kavanagh, D. Leech, *Phys. Chem. Chem. Phys.* **2013**, *15*, 4859.

[21] I. Osadebe, D. Leech, *ChemElectroChem* **2014**, *1*, 1988.

[22] I. Osadebe, P.Ó Conghaile, P. Kavanagh, D. Leech, *Electrochim. Acta* **2015**, *182*, 320.

[23] S. Tsujimura, K. Murata, W. Akatsuka, *J. Am. Chem. Soc.* **2014,** *136*, 14432.

[24] E. Tremey, C. Stines-Chaumeil, S. Gounel, N. Mano, *ChemElectroChem*, **2017***, 4*, 2520.

[25] R. Kumar, D. Leech, *Bioelectrochem.* **2015**, *106*, 41.

[26] R. Kumar, D. Leech, *J. Electrochem. Soc.* **2014**, *161*, H3005.

[27] E.M. Kober, J.V. Caspar, B.P. Sullivan, T.J. Meyer, *Inorg. Chem.* **1988**, *27*, 4587.

[28] R.J. Forster, J.G. Vos, *Macromolecules* **1990**, *23*, 4372.

[29] D. MacAodha, P.Ó Conghaile, B. Egan, P. Kavanagh, D. Leech, *ChemPhysChem* **2013**, *14*, 2302.

[30] C. A. Burtis and E. R. Ashwood (eds.), *Tietz Fundamentals of Clinical Chemistry* W. B. Saunders Co., Philadelphia, Pennsylvania, 4th ed., **1996**.

[31] C. Taylor, G. Kenausis, I. Katakis, A. Heller, *J. Electroanal. Chem.* 1995, 396, 511.

[32] P.N. Bartlett, K.F.E. Pratt, *J. Electroanal. Chem.* 1995, 397, 61.

[33] B.T. Limoges, J. Moiroux, J.-M. Savéant, *J. Electroanal. Chem.* 2002, 521, 8.

[34] B. Qi, X. Chen, F. Shen, Y. Su, Y. Wan, *Ind. & Eng. Chem. Res.* **2009**, *48*, 7346.

[35] E.J. Calvo, C. Danilowicz, L. Diaz, *J. Chem. Soc., Faraday Trans.* **1993**, *89*, 377.

[36] G. Chen, J. Chen, C. Srinivasakannan, J. Peng, *Appl. Surf. Sci.* **2012**, *258*, 3068.

[37] A. Prévoteau, N. Mano, *Electrochim. Acta* **2012**, *68*, 128.

[38] H.-H. Kim, N. Mano, Y. Zhang, A. Heller, *J. Electrochem. Soc.* **2003**, *150*, A209.

[39] V. Soukharev, N. Mano, A. Heller, *J. Am. Chem. Soc.* **2004**, *126*, 8368.

[40] N. Mano, *Chem. Comm*. **2008**, 2221.

[41] E. Magner, *Analyst* **2001**, *126*, 861.

[42] V. Coman, R. Ludwig, W. Harreither, D. Haltrich, L. Gorton, T. Ruzgas, S. Shleev, *Fuel Cells* **2010**, *10*, 9.

[43] C. Kang, H. Shin, Y. Zhang, A. Heller, *Bioelectrochem.* **2004**, *65*, 83.

[44] A.C. Guyton, J.E. Hall, *Textbook of Medical Physiology*, 11th ed., Elsevier Saunders, Philadelphia, PA, **2006**.

[45] P. Ó Conghaile, M. Falk, D. MacAodha, M.E. Yakovleva, C. Gonaus, C.K. Peterbauer, L. Gorton, S. Shleev, D. Leech, *Anal. Chem*. **2016**, *88*, 2156.

[46] M. Cadet, S. Gounel, C. Stines-Chaumeil, X. Brilland, J. Rouhana, F. Louerat, N . Mano, *Biosens. & Bioelectron.,* **2016,** *83*, 60.